Title

Exploring protein solution structure: Second moments of fluorescent spectra report heterogeneity of tryptophan rotamers

Authors

Gasymov, Oktay K
Abduragimov, Adil R
Glasgow, Ben J

Publication Date

2015-11-01

DOI

10.1016/j.saa.2015.06.043

Peer reviewed

HHS Public Access

Author manuscript

Spectrochim Acta A Mol Biomol Spectrosc. Author manuscript; available in PMC 2016 November 05.

Published in final edited form as:

Spectrochim Acta A Mol Biomol Spectrosc. 2015 November 5; 150: 909–920. doi:10.1016/j.saa.2015.06.043.

Exploring Protein Solution Structure: Second Moments of Fluorescent Spectra Report Heterogeneity of Tryptophan Rotamers

Oktay K. Gasymov, **Adil R. Abduragimov**, and **Ben J. Glasgow**

Departments of Pathology and Ophthalmology and Jules Stein Eye Institute, University California at Los Angeles, CA 90095

Abstract

Trp fluorescent spectra appear as a log-normal function but are usually analyzed with λ_{max}, full width at half maximum, and the first moment of incomplete spectra. Log-normal analyses have successfully separated fluorescence contributions from some multi-Trp proteins but deviations were observed in single Trp proteins. The possibility that disparate rotamer environments might account for these deviations was explored by moment spectral analysis of single Trp mutants spanning the sequence of tear lipocalin as a model. The analysis required full width Trp spectra. Composite spectra were constructed using log-normal analysis to derive the inaccessible blue edge, and the experimentally obtained spectra for the remainder. First moments of the composite spectra reflected the site-resolved secondary structure. Second moments were most sensitive for spectral deviations. A novel parameter, derived from the difference of the second moments of composite and simulated log-normal spectra correlated with known multiple heterogeneous rotamer conformations. Buried and restricted side chains showed the most heterogeneity. Analyses applied to other proteins further validated the method. The rotamer heterogeneity values could be rationalized by known conformational properties of Trp residues and the distribution of nearby charged groups according to the internal Stark effect. Spectral heterogeneity fits the rotamer model but does not preclude other contributing factors. Spectral moment analysis of full width Trp emission spectra is accessible to most laboratories. The calculations are informative of protein structure and can be adapted to study dynamic processes.

Graphical Abstract

Correspondence to: Oktay K. Gasymov and Ben J. Glasgow: ogassymov@mednet.ucla.edu; bglasgow@mednet.ucla.edu. Oktay K. Gasymov, 100 Stein Plaza, Rm# B267, Los Angeles, CA 90095. Phone: (310) 825-6261; Fax: (310) 794-2144; ogassymov@mednet.ucla.edu
Adil R. Abduragimov, 100 Stein Plaza, Rm# B267, Los Angeles, CA 90095. Phone: (310) 825-6261; Fax: (310) 794-2144; aabdouraguimov@mednet.ucla.edu
Ben J. Glasgow, 100 Stein Plaza, Rm# B269, Los Angeles, CA 90095. Phone: (310) 825-6998; Fax: (310) 794-2144; bglasgow@mednet.ucla.edu

Conflict of Interest Statement: The authors declare no competing financial interests.

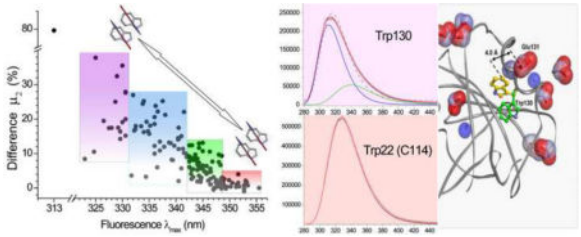

Keywords

site-directed tryptophan fluorescence; rotamer heterogeneity; fluorescence spectral moments; tear lipocalin; β-lactoglobulin; *Plasmodium falciparum triosephosphate isomerase* (PfTIM); Human serum albumin

Introduction

Spectroscopic techniques are especially important to probe protein structure for dynamic information that cannot be derived from X-ray crystallography. Flexible regions may be poorly resolved in crystallography. Precise rotamer distributions may be especially difficult to determine. Often crystallization of the native protein is unsuccessful.

Trp can be used as effective probe in fluorescence, CD, resonance Raman, absorption, etc. [1–8]. Burstein's group and others effectively characterized tryptophan fluorescence spectra as a log-normal distribution that could be derived from maximum position (λ_{max}) and amplitude (intensity) for spectra of tryptophan derivatives in solvents [9–14]. Algorithms for fitting with log-normal analysis permitted deconvolution of multi-tryptophan fluorescence spectra of proteins into individual components [9–11]. Seventeen of the 48 proteins used in assignment of fluorescence λ_{max} had only one tryptophan. Only 9 of these 17 proteins showed a single log-normal component. Deviations from a single log-normal component of fluorescence of single Trp residues were attributed to incomplete purification of protein from bound ligand, incomplete dimerization, different conformers of Trp from isomerization of Pro, or regarded as an inexplicable discrepancy [11]. Here, we consider the possibility that the deviations are due at least in part to rotamer distributions of tryptophan that manifest heterogeneous fluorescence properties. The rationale is that large red shifts observed for exposed Trp residues arise from the Stark effect mainly produced by the dipoles of water molecules [15–18]. Each rotamer of a given Trp may reside in disparate exposed and buried environments creating spectral heterogeneity. Since the log-normal distribution is inherently positively skewed toward the red edge of the spectrum, the spectral width is likely to be more sensitive to the Stark effect than λ_{max}. To calculate true spectral width and subsequently spectral moments of all blue shifted Trp's in proteins the entire Trp spectrum is required. The blue region from 280–305 nm is unavailable due to overlap of the excitation and emission. The inaccessible blue region can be modeled and extrapolated. Here, the experimental spectrum was fit to a log-normal function with multiple parameters if necessary. A composite spectrum was then constructed, composed of 280–305nm extrapolated from the fitting curve and 306–500nm from the original experimental spectrum. Moment analysis of the composite spectrum could then be compared to the elementary log-

normal spectrum derived simply from the λ_{max}. The reason for using a composite spectrum rather than an experimental spectrum fit to multiple log-normal components is the uncertainty associated with multiple parameters that could arise in the skewed but informative red edge of the spectra. The availability of a complete set of single tryptophan mutations in one protein, tear lipocalin, in concert with verified crystallographic and solution structure data provided an ideal testing platform [6, 19]. Further, structural constraints imposed by specific rotamers in these mutations provided key corroboratory data [20, 21]. The work was further validated in other proteins for which rotameric heterogeneity is known.

Results

Characterization of the simulated "elementary" log-normal components for tryptophan fluorescence spectra

Figure 1 shows the simulated "elementary" log-normal fluorescence spectra of Trp with various λ_{max} values using formula 1 [9]. This formula well characterizes the spectra of NATA in various solvents [18, 22–24]. The blue shift decreases the bandwidth of the spectrum consistent with the observed fluorescence spectra of Trp in solvents of various polarities as well as in proteins. Only one parameter, λ_{max}, is needed to characterize these spectra of pure Trp derivatives within a wide range of fluorescence λ_{max}.

One of the parameters of the log-normal distribution is an asymmetry (skewness) parameter. The positive skew increases with a blue shift of the fluorescence λ_{max} (Figs. 1 and S1). The first moment does not report the highest intensity value (λ_{max}) but rather a barycenter, i.e., the amplitude-weighted average wavelength of the spectrum [25]. The first moments of the simulated spectra linearly depend on fluorescence λ_{max} (Fig. S1). Second moments characterize spectral breadth of the spectra. Second moments are higher for the red shifted fluorescence spectra, but the dependence is not linear (Fig. S1). Qualitatively, this feature is evident from the simulated log-normal components (Fig. 1).

Solving for best fit parameters *A*, *B*, and *t* revealed $A = (5.1 \pm 0.1) \times 10^{-4}$; $B = 502.4 \pm 37.8$; $t = 25.36 \pm 0.16$ in simulated spectra. These parameters will allow computation of the second moments of elementary log-normal components for any λ_{max} value. Comparison of the second moments in single tryptophan fluorescence spectra of proteins will determine the rotamer heterogeneity at a specific site.

Characterization of spectral moments of Trp spectra in the protein

The pattern produced by the plot of the first moments of the composite Trp spectra along the sequence reveals the site-resolved secondary structure of the protein, TL (Fig. 2). The β-strand regions demonstrate alternating periodicity for the first moments. The main α-helical region of TL shows a periodicity of 3.6 for the variation of the first moments plotted sequentially (red colored symbols in Fig. 2). The pattern observed for the first moments in Figure 2 is very similar to that observed previously for the fluorescence λ_{max} [6].

The pattern of the second moments of Trp spectra of TL (Fig. S2) appears similar to that observed for the first moments. However, the alternate periodicities of the β-strands

observed for λ_{max} or μ_1 values are altered for the second moments of strands A, C and D (Fig. S2). Comparison of the μ_1 and μ_2 values (Figs. 2 and S2) indicates that the alteration is not uniform. In the β-strand A, alternate periodicity (residues from 17 to 25) is obscured. In strand C, distortion of the pattern is evident for position 55 (Fig. S2). Strand D seems to show alternate periodicity for μ_2 values. However, the differences in μ_2 values for positions 67–71 are blunted (Fig. S2). These changes result from heterogeneous Trp rotamer environments.

Rotamer heterogeneity

Spectral heterogeneity cannot be properly characterized by the absolute values of second moments, because second moments depend on fluorescence λ_{max}. However, the difference in second moments of the composite and simulated spectra can be normalized to the second moment of a corresponding log-normal component. This parameter, coined rotamer heterogeneity or $\Delta\mu_2$, does not depend on fluorescence λ_{max} and is a unique property of the spectrum. Rotamer heterogeneity values of Trp spectra in TL are shown as a distribution in Figure 3. The values tend to be higher for blue shifted fluorescence λ_{max}. However, essentially ”elementary” log-normal spectra ($\Delta\mu_2$ values close to 0) are observed with fluorescence λ_{max} values up to 332 nm (Fig. 3). The rotamer heterogeneity values are plotted progressively along the amino acid sequence of TL in Figure 4. At first glance, the periodicity of rotamer heterogeneity appears inverted compared to the first moments (Figs. 2 and 4). Rotamer heterogeneity is lower for exposed sites, i.e. the red shifted fluorescence λ_{max}. The fluorescence spectrum of Trp130 shows the highest rotamer heterogeneity observed in TL. This spectrum is also the most blue-shifted among all sites of TL. The periodicity pattern of $\Delta\mu_2$ is retained only for the β-strands B, C, D, E and G. Where rotamer heterogeneity diverges from first moments, important structural alterations in periodicity are evident (Figs. 2 and 4). Two β-strands A and F show “distorted” patterns for $\Delta\mu_2$ that also contain two conserved β-bulges (positions 20 and 21 in A and 89 and 90 in the F), (Fig. 2). Thus, the pattern of the rotamer heterogeneity is not simply an inverted replica of that observed for the first moments but contains new information.

Structural features revealed by rotamer heterogeneity of Trp fluorescence

The amino acid sites with the highest rotamer heterogeneity are insightful (Fig. 5). These sites, 19, 41, 77, 91 and 116, reside at similar depths in the barrel of TL. Sites 55 and 83 show high heterogeneity but are positioned at the tips of the β-strands C and F at the open end of the barrel. Trp83 has a first moment at about 348 nm, connoting a limited exposure to the solvent. Trp83 resides at the fulcrum for the shortest connecting loop EF in TL. The mobilities of the backbone and side chain of Trp83 are restricted. The mobility of site 55 is restricted by the nearby disulfide bond (Fig. 5).

The averages of rotamer heterogeneity values were calculated for the secondary structure elements of TL (Fig. 6). The β-strand D forms the horizontal edge of the barrel. Strand D shows the lowest rotamer heterogeneity value, 6.1 (Figs. 4 and 6). Strands A and H show the highest average rotamer heterogeneity values, 18.2 and 17.3 respectively. These strands also contain sites that show the lowest isotropic displacement values (Fig. 6, lower portion of the figure).

Interrogation of the features that generate site-specific rotamer heterogeneity

To determine the influence of an adjacent charged group on the rotamer heterogeneity of Trp spectra, Lys114 was substituted with Cys in the mutant W22 (W22C114). A positive charge of the side chain of Lys114 positioned near the benzene ring of the indole of Trp22 (Fig. 7) produces a significant red shift in the fluorescence spectrum (Fig. 2, blue solid square at 22 and letter M). This spectral shift is also evident for λ_{max} values [6]. The red shift created by Lys114 results in distortion of the expected periodicity of the β-strand (Fig. 2). Substitution of Lys114 with Cys produces a considerable hypsochromic shift of the first moment of the spectrum for Trp22 from 352.4 nm to 338.4 nm. The blue shift produced by removal of the charged side chain results in an alternating periodicity pattern of the β-strand A (Fig. 2, blue solid triangle at 22 and letter M^*). The solution structure revealing the interaction of Lys114 was confirmed later by X-crystallography of TL [6, 19]. However, the rotamer heterogeneity derived from the second spectral moments for W22 and W22C114 are minimally different, 13.2 and 16, respectively. In this particular situation, although the nearby charged group influences the rotamer heterogeneity of Trp fluorescence, the response is less than the change observed for the first moments. Thus, underlying attributes that determine the magnitude of the fluorescent shift are different from those that determine the rotamer heterogeneity (Figs. 2 and 6).

The positions of the charged groups around the rotamers of Trp130 are shown in Fig. 8. Indicated rotamers of Trp130 are based on previous fluorescence lifetime data [20]. The charged atom of Glu131 is located adjacent to the benzene part of the indole in the *t*-rotamer. The relative position of this atom is changed significantly in the g^- rotamer (Fig. 8).

Spectra heterogeneity is exemplified when the composite fluorescence spectra of Trp22 (C114) and Trp130 are compared to their log-normal component analysis (Fig. S3). The rotamer heterogeneity calculated for spectra of Trp22 (C114) and Trp130 are markedly different (Fig. 4). A single “elementary” log-normal component is adequate to characterize the fluorescence spectra of Trp22 (C114) with relatively low heterogeneity. The fluorescence spectrum of Trp130 requires two log-normal components for satisfactory fitting (Fig. S3).

Effect of altered long-range interactions on rotamer heterogeneity

The side chains of residues V113 and L115 have long-range interactions with that of Trp130 [6, 19, 20]. The substitutions of either or both sites simultaneously have been shown to greatly change the fluorescence parameters of Trp130 [21]. As shown in Fig. 9, modification of the long-range interaction sites of Trp130 affects fluorescence λ_{max} and rotamer heterogeneity. In general $\Delta\mu_2$ decreases are associated with bathochromic shifts in λ_{max}. Despite reductions in fluorescence λ_{max} values for the mutants W130G113 and W130A115, their rotamer heterogeneity values are very close. In contrast, mutants W130F113F115 and W130F115 show identical fluorescence λ_{max} values but their respective rotamer heterogeneities are different.

Validation of parameters in other proteins with known crystal or solution structures

Published spectra were complete enough to apply moment analysis to β-lactoglobulin, human serum albumin, and *Plasmodium falciparum triosephosphate isomerase* (PfTIM).

Bovine β-lactoglobulin—The fluorescence spectrum of the β-lactoglobulin has a maximum around 332.5 nm (Fig. S4A), is similar to Trp17 of TL [6]. Second moment analysis performed for β-lactoglobulin from two separate literature data shows almost identical $\Delta\mu_2$, i.e., rotamer heterogeneities (Table 1).

Human serum albumin—For human serum albumin the fluorescence spectra of Trp124 show higher heterogeneity values at pH 2.0 and 4.1 (27 and 28, respectively) compared to spectra at pH 7.0 and 9.0 (15 and 17, respectively) (Table 1). These data match the fluorescence decay properties of Trp124. The average contributions of the fluorescence lifetime components to the steady-state fluorescence (calculated from Table 1 of reference [26] spectra indicate that long lifetime components (7.51ns and 6.55 ns) are dominant at pH 7.0 and 9.0 (91% and 93%, respectively) (Table 2). Contributions of the short life component are just 0.2% and 0.6% at pH 7.0 and 9.0, respectively. However, at pH 2.0 and 4.1, contributions of medium and short lifetime components to the steady-state spectra are higher, i.e. spectra are more heterogeneous.

PfTIM—PfTIM contains two tryptophan residues, Trp11 and Trp168 for which single Trp mutants show similar blue shifted emission λ_{max} values, 333 and 329 nm, respectively (Fig. S5) [27]. Rotamer heterogeneity values for both are increased; Trp168 is unusually high, 72, compared to 43 for the buried Trp11.

Discussion

The key findings of this work are: 1) the second moment reflects the full width of the Trp spectra and is much more sensitive to spectral heterogeneity. 2) Sequential second moments provides additional site-specific structural details e.g. β bulges, but also show asymmetry of rotamers at these sites. 3) A parameter, coined rotamer heterogeneity, reflects the deviation in the environment of Trp at a particular site from that of a corresponding isotropic solvent (“elementary” log-normal component for the emission spectrum). The rotamer heterogeneity value probably indicates disparate electric field projections of individual tryptophan rotamers and their interactions with individual side chains as well as strands.

Properties and limitations of λ_{max} and full width at half maximum (FWHM in Trp spectra

The λ_{max} and first moment provide an overview of secondary structure in solution. The FWHM gives a crude assessment of spectral heterogeneity. But red-shifted components of small-amplitude, will not contribute to FWHM. Fluorescence λ_{max} values correlate with secondary structural features, related to solvent exposure of the Trp sites of proteins. Deviations from “elementary” log-normal components are not necessarily reflected in the λ_{max}. Tryptophan spectra may yield the same λ_{max} but have different spectral widths.

Trp fluorescence log-normal distribution for analysis of protein structure

The basis of the log-normal distribution is related to the complexity of probability distributions over energy states and the Frank-Condon principle [28, 29]. Widths of the fluorescence (or second moment) spectra are proportional to the slope of the ground state potential around fluorescence λ_{max} [28]. The shapes and position of the band are determined by changes in molecular geometry upon excitation [29].

Trp composes about 1.2 % and 3.3 % of soluble and membrane proteins, respectively [30]. Trp fluorescence shows a wide distribution for λ_{max} values relevant to solvent exposure (Fig. 10). In log-normal analysis of 150 different proteins, the number of native proteins with buried versus exposed tryptophans was approximately equal [13]. However, if one considers every possible amino acid site in a single protein (TL) for tryptophan then a different perspective emerges (Fig. 10). The fluorescence λ_{max} distribution in TL shows that most amino acid residues are solvent exposed. Yet, the one native tryptophan is buried in the hydrophobic core of TL [6]. Trp at this position is very conserved throughout the lipocalin family [31, 32] and plays important role in structural stability and ligand binding [33]. In this family of proteins there seems to be a functional or biologic bias for the native tryptophan at a buried residue [30]. This bias toward buried tryptophans should prevail in most soluble proteins that contain a cavity [6]. Therefore, log-normal analysis of Trp in proteins is a rational approach but in some cases Trp spectra analysis are not adequately described by a single log-normal component or characterized adequately by λ_{max} values. Multi-component introduces additional uncertainties.

First moment of a spectrum (or center of spectral mass) preserves secondary structural features of protein

Previously, the center of spectral mass, μ_1, was shown to be a more accurate parameter to quantify spectral shifts than λ_{max} [25]. However, this application of $\mu_1$was subject to limitations. First, the study of μ_1 was limited to a single oligomeric protein with multiple tryptophans. Second. the derivation did not use the full width of spectra because the excitation wavelength of Trp at 295 nm necessitates the truncation on the blue side of the emission spectrum. Third, comparison of μ_1 with other proteins is limited because spectral shifts may not be accounted for without the full spectral width. To vitiate these limitations, here, the blue side of the spectrum was extrapolated with log-normal analysis to obtain the entire spectral width. The first moment as calculated appears quite good for a monomeric protein with a single Trp. The first moments of Trp fluorescence reveal side chains that alternate between solvent exposed and buried inside the barrel (Fig. 2). For fluorescence Trp spectra with rotamer heterogeneity, first moments have higher values compared to those of the corresponding “elementary” log-normal spectra (Fig. S6). However, despite the wide range of rotamer heterogeneity observed in TL (Fig. 4), the distribution pattern for the first moments preserves the information for site-specific secondary structure of TL that was educed from fluorescence λ_{max} and later confirmed by X-ray crystallography [6, 19]. Data obtained from TL (Fig. S6), indicate that single Trp fluorescence λ_{max} measurements around 325 nm will produce up to about a 3 nm difference in the first moments. The fluorescence spectra with first moments in the 335–338 nm range may produce the same λ_{max} at 325 nm (Fig. S6). Increased sensitivity is the advantage of analysis of the first moment over λ_{max}.

Second moments are sensitive to spectral heterogeneity

The λ_{max} and μ_1 values of TL can be compared to that of corresponding "elementary" log-normal components (Fig. S6) for Trp fluorescence spectral heterogeneity. The λ_{max} and μ_1, are less sensitive than second moments to heterogeneous populations of rotamers. The pattern observed for the second moments of Trp spectra appears different (Fig. S2) compared to that of the first moments (Fig. 2) or λ_{max} values [6]. The basis for this apparent discrepancy is revealed by calculation of rotamer heterogeneity.

Spectral (rotamer) heterogeneity of Trp spectra reflects dissimilar rotamer components

The basis for fluorescence lifetimes of excited state, quantum yield, and quenching is well studied [34–39]. Fluorescence lifetimes of conformationally restricted peptides show that the electron transfer mechanism of quenching depends on the rotamer conformations of Trp [37, 40–42]. Single tryptophans in proteins usually show at least two lifetimes that can be linked to the rotamer states [20, 41, 42]. Rotamer populations are reflected in Trp fluorescence lifetimes in TL [20, 21]. Trp residues introduced to the main α-helix sites of TL indicated only two lifetimes [20, 21]. Restriction to two lifetimes is congruous with steric restraints that allow Trp to assume only two χ_1 rotamers (−60, 180) out of three (−60, 180, +60). The positions of the charged groups relative to the indole-amide system can significantly change lifetimes of the rotamers. The side chains of eight amino acids can effectively quench Trp fluorescence [35]. Gln, Asn, Glu, Asp, Cys, and His quench Trp fluorescence by an excited state electron transfer mechanism [35]. However, quenching works through an excited state proton transfer mechanism for the side chains of Lys and Tyr [35]. The charged residues (both negative and positive) may quench (or un-quench) Trp fluorescence indirectly. The electric field strength and direction plays a major role in electron transfer from indole ring to the nearest carbonyl group via stabilization or destabilization of CT (the charge transfer state) [18, 23, 43]. Another group assigns multiple fluorescence lifetimes of Trp to substructures of proteins [44–47]. However, a detailed description of the substructures that yield different lifetimes remains to be shown. The description of the spectral heterogeneity is not tied to but fits the rotamer model.

Reduced rotamer heterogeneity for red-shifted emissions (Fig. 4) is explained by the mobile solvent dipoles that surround side chains in exposed sites. Fast rearrangement of the solvent molecules results in efficient minimization of the excited energy level of every rotamer of Trp. In sites where side chain motion is restricted and also shielded from solvent molecules the rotamer heterogeneity is higher. Given the abundant information on Trp fluorescence in proteins [1, 17, 35, 36, 38, 40, 42, 48–51] as well as on TL [6, 20, 21, 52–55], it is reasonable to speculate that the rotamer heterogeneity of a single Trp spectrum can be mainly attributed to the rotamer population, mainly χ_1 rotamers. Each rotamer is assigned by their distinct fluorescence lifetime and calculated spectral components [37, 38, 41, 42, 48, 56, 57]. Rotamer heterogeneity originates from the rotamer spectral components, but not all multi-rotamer spectra show rotamer heterogeneity. For example, the fluorescence of Trp in the main α-helix as well as in the loops AB, CD and EF show at least two lifetimes [20, 52, 55]. However, rotamer heterogeneity values for these sites vary from 0 to the maximum value of 79. Fluorescence lifetimes of rotamers may drastically differ without associated spectral heterogeneity. The internal Stark effect [17, 48, 51] can be applied to the rotamers

of Trp. The charge distributions with respect to the rotamers may induce the site-specific rotamer heterogeneity of Trp fluorescence. For example, the deeply buried sites with blue shifted Trp fluorescence show the greatest rotamer heterogeneity (Fig. 4). Only two sites, (126 and 130) of the main α-helix, show significant rotamer heterogeneity. The side chains of 126 and 130 of the main α-helix face the β-strand H where tertiary interactions occur [6, 19, 21]. Modification of the interaction sites changes the rotamer heterogeneity (Fig. 9). In the loop AB, the heightened rotamer heterogeneity at sites (30, 34 and 35) (Figs. 4 and 5) can be explained by restriction in backbone mobility; the side chains point the inside of the cavity. Backbone restriction is requisite, but by itself is not enough to produce high rotamer heterogeneity (e.g. side chain at site 33). The electric field projection on the indole ring must be altered in the process of switching from one rotamer state to another to show an appreciable degree of rotamer heterogeneity in the composite spectrum.

Trp124, positioned just beyond the N-terminal portion of the α-helix, demonstrates a high rotamer heterogeneity value in concordance with data from low-temperature site-directed CD of TL [58]. Marked enhancement of the ^1L_b CD band at low temperature for Trp124 was consistent with a high degree of rotamer population rearrangement, i.e. conformational mobility. Significant spatial displacement was observed for position 124 in the apo- to holo-transition for these crystal forms of TL [19, 59].

The fluorescence spectrum of Trp130, shows the highest $\Delta\mu_2$ value. The fluorescence decay of Trp130 is characterized by two lifetimes linked to two rotamers (*t*- and g^-) *c*onsistent with constraints imposed by the backbone of the α-helix. [20]. The g^+-rotamer was sterically excluded. The rotamers of Trp130 and surrounding charged residues in TL are shown in Figure 8. The spatial distribution of the charged residues suggests that negatively charged Glu131 is a dominant factor for the spectral shift of Trp 130. A negative charge near the benzene ring of an indole induces a hypsochromic shift in fluorescence spectra. This is the case for the *t*-rotamer of Trp130. However, the relative orientation of these groups reduces the effective negative charge in the g^--rotamer. The spectrum of the g^--rotamer is expected to be significantly red shifted compared to that of the *t*-rotamer (Fig. S3). This situation creates a high $\Delta\mu_2$ value for the spectrum of Trp130. The electric field projection on the indole of Trp should be asymmetric for the rotamers to produce significantly shifted components and a high $\Delta\mu_2$ value. Therefore, in some significantly blue shifted Trp spectra with symmetric electric field projections, the rotamer heterogeneity value is minimal (Figs. 2, 4 and 8). The rotamer heterogeneity value discriminates the types of environments at the specific site where Trp is introduced.

Average rotamer heterogeneity values reflect unique strand positions and interactions

The rotamer heterogeneity of Trp spectra can also be used for characterization of the regions of the assigned secondary structure of the protein (Fig. 6). The β-strands A and H show the highest average rotamer heterogeneity values and are conserved in the lipocalin family. The β-strand A forms the closed-end of the barrel. The A strand has a β-bulge that bends to interact with the β-strands H and I. In addition, both the β-strands A and H interact with the main α-helix of the protein (Fig. 6). These structural features indicate restricted backbone mobility of the strands. Indeed, the mean isotropic displacement values are the lowest for the

sites of the β-strand A and H (Fig. 6, lower part). The β-strand D with the lowest average rotamer heterogeneity forms the edge of the barrel. One side of the strand D is stabilized by the interaction with the neighboring β-strand C. The first moments of the Trp fluorescence spectra at the sites of the β-strand D show only minimal differences for alternating periodicity (Fig. 2).

Validation of rotamer heterogeneity in other proteins with known crystal or solution structures

Bovine β-lactoglobulin—The data demonstrate the consistency of rotamer heterogeneity values among Trp residues in analogous positions of structurally similar proteins (Fig. S4 and Table 1). Bovine β-lactoglobulin shares 23% sequence identity with TL and their structures are very similar [6] (Fig. S4). Trp19 is analogous to Trp17 of TL and is located in a conserved position in the binding barrel. The Arg124 is analogous to Arg118 of TL and is located at the closed end of the barrel. These conserved Trp-Arg pairs of the lipocalin family stabilize structures via cation-π interactions [60]. Although bovine β-lactoglobulin has two Trp residues, only Trp19 accounts for Trp fluorescence [44]. Rotamer heterogeneity values are consistent for these structurally similar lipocalins.

Human serum albumin—Human serum albumin (HSA) transports a variety of fatty acids and drugs in the circulatory system. The protein undergoes multiple conformational transitions by changes of pH values. In HSA, fluorescence parameters of single Trp214 are sensitive to these conformational transitions [26]. Steady-state and time-resolved fluorescence spectroscopy as well as time-resolved area-normalized fluorescence emission spectra (TRANES) indicate that the microenvironment around Trp214 is tightly packed at both acidic and basic pH although the entire conformation is relaxed [26]. Fluorescence decay and TRANES properties at various pH values suggest that a rotamer/conformer model is suitable for Trp124 fluorescence. The heterogeneity values of HSA at various pH values (Fig. S7) corroborate the model (Table 1). Rotamer heterogeneity substantiates the rigidity of a specific Trp side chain, despite concurrent global relaxation. The findings are in a very good agreement with another study, in which the fluorescence lifetime of Trp 124 of HSA was measured at various pH values [61]. Calculation of their data with the fluorescence lifetime parameters shown in their Table 1 of reveals fractional contributions ($f_i = a_i \tau_i / \Sigma a_j \tau_j$) of the longest lifetime (7.2–7.8 ns) to the steady-state fluorescence of 86% at both pH values of 4 and 7.5. Accordingly, the DAS (decay associated spectra) of the longest lifetime shows the dominant contribution to the total spectrum.

PfTIM—In PfTIM the elevated rotamer heterogeneity values of 72 and 43 for Trp 178 and 11 (Table 1), respectively invite comparison to TL. The only residue in TL that had a similar heterogeneity value (80) was Trp130. The side chain of Trp130 is in very restricted environment and relative position of the charged group of G131 drastically differ in *t*- and *g*-rotamers (Fig. 8). The crystal structure of PfTIM reveals the origin of the high heterogeneity value and unusually blue-shifted fluorescence of Trp168 in a polar environment (Fig. S8). Trp168 is surrounded by polar groups, suggesting specific electrostatic effects may account for the blue shift in fluorescence [27]. The side chain of Arg134 makes a cation-π interaction with the pyrrol ring of Trp 168 (Fig. S8A). This interaction stabilizes electron

density at the pyrrol ring, to produce a blue shift in fluorescence λ_{max}. However, in the alternative rotamer conformation (Fig. S8B) of Trp168 (*t*- rotamer) the side chain of Lys174 is located at the benzene side of the Trp and makes cation-π interaction. This interaction stabilizes electron density at the benzene ring of Trp to produce a red shift in fluorescence λ_{max}. Two alternate conformers of Trp 168 produce both blue- and red-shifted fluorescence that yield a highly heterogeneic fluorescence spectrum. Thus, high rotamer heterogeneity values predict the environment for Trp168 that corroborates the crystal structure of the protein. The side chain of Trp11 of PfTIM is surrounded by both hydrophobic as well as hydrophilic residues (Fig. S9). The charged group of the Lys12 is located at the pyrrol side of Trp11, but located at distance of 10.2 Å (CD1(Trp11) and NZ(Lys12)). At this position Lys12 may somewhat contribute to a blue-shift of the fluorescence. Therefore, the influence of Lys12 to the fluorescence spectrum of Trp11, as well as the heterogeneity value will be much less compared to that of Arg134 and Lys174 to Trp168. Indeed, the heterogeneity value for Trp11 is quite high (43) but substantially less compared to that of Trp168 (72). Overall, the rotamer heterogeneity values coincide with the structural features imposed on two tryptophans.

In this paper, inhomogeneous spectral broadening is attributed to rotamer heterogeneity. An argument can be made that solvent relaxation can also contribute to the spectral broadening, which may increase fluorescence lifetimes at the red side of the Trp spectra [62]. But multiple rotamer populations produce the same phenomena [37]. Because our prior work shows that the rotamer assignments correlate with fluorescent lifetimes in restricted sites it follows that high heterogeneity values are mainly derived from the rotamer mechanism [20, 21, 58]. Contributions from differences in solvent relaxation for various conformational isomers of Trp would be consonant with our results.

Conclusion

The applicability of the full width second moments and rotamer heterogeneity was validated for proteins from structurally diverse classes with known crystal or solution structures. The method will facilitate the evaluation of spectral changes that reflect structural features during unfolding, ligand binding, high pressure, pH titration, etc. Straightforward computations and simple laboratory equipment are all that is needed. The tools are readily available to most laboratories to investigate protein structure.

Materials and Methods

Site-directed mutagenesis and plasmid construction

The exon of TL (lipocalin-1, LCN1), bases 115-592, was cloned into pET 20b (Novagen, Madison, WI) [63] to generate cDNA [64]. Flanking sequences for Ndel and BamHI restriction sites were added to produce the native protein sequence with retention of the initiating methionine [65]. The TL mutant, W17Y [33], was the template to construct single tryptophan mutants. Most of the mutant proteins were produced using polymerase chain amplification with primer extension [6]. However, some mutants plasmids were constructed with oligonucleotides (Invitrogen) using the QuikChange II site-directed mutagenesis kit (Stratagene). cDNAs with the introduced point mutations were sequenced. Amino acid 1

corresponds to His, bases 115-117 [63]. Trp was introduced sequentially to make 155 mutant proteins each with a single tryptophan in TL. For simplicity, the names for the mutants were abbreviated as W17Y/L19W (W19). The fluorescence data for W117 are not presented because expression has yielded only oligomeric protein [6]. The mutant M22W/K114C, was constructed to show the influence of the positive charge of K114 on the fluorescence of W22. All mutant proteins have the native fold as previously shown by far-UV circular dichroism [6, 20]. The perturbations observed in Trp mutation at distinct sites were attributed to changes in packing of secondary structural elements [6, 66]. The effect of destabilization of long-range interactions on the second moment of the fluorescent spectrum was investigated. Specifically, the following mutants were produced to alter the interaction of Trp 130 with amino acids side chains at 115 and 113: W130G113, W130A115, W130G115, W130F115 and W130F113F115.

Expression and purification of mutant proteins

The plasmids of the mutants were transformed in E. Coli, BL 21 (DE3). Cells were cultured and proteins were expressed, purified, and analyzed as described [6, 55]. The expressed mutant proteins were used without additional enrichment with ligand. As shown previously, mutant proteins of TL expressed in E. Coli as well as the native protein purified from tears contain a similar array of lipid ligands including palmitic acid [33, 67, 68]. Concentrations of the mutant proteins were determined using the molar extinction coefficient of TL (ε_{280}= 13760 $M^{-1}cm^{-1}$) [69]. The far UV CD spectra for each mutant protein was performed as previously published [6, 21].

Absorption Spectroscopy

UV absorption spectra of the single Trp mutants of TL were recorded at room temperature using a Shimadzu UV-2400PC spectrophotometer. The buffer was 10 mM sodium phosphate, pH 7.3.

Fluorescence spectroscopy

Fluorescence measurements were made on a Jobin Yvon-SPEX Fluorolog-3 spectrofluorometer; bandwidths for excitation and emission were 2 nm. The excitation λ_{max} at 295 nm provided selective absorption by Trp compared to other aromatic amino acids. Protein solutions with absorbance of about 0.05–0.07 at 295 nm were used. All spectra were obtained from samples in 10 mM sodium phosphate, pH 7.3, at room temperature. The fluorescence spectra were corrected for light scattering from buffer and the instrument response function using the correction curve provided by Jobin Yvon.

Comparison of single Trp fluorescence spectra in proteins to corresponding “elementary” log-normal components

“Elementary” log-normal fluorescence spectra were constructed using the following formula [9].

$$I(\lambda)=I_m\exp\left[-\frac{\ln 2}{\ln^2 p}\ln^2\left(\frac{(a-1/\lambda)}{a-1/\lambda_m}\right)\right] \quad (1)$$

where $I_m = I(\lambda_m)$ is the maximal fluorescence intensity; λ_m is the wavelength of the band maximum; $p = (1/\lambda_m - 1/\lambda_-)/(1/\lambda_+ - 1/\lambda_m)$ is the band asymmetry parameter (skewness); $a = 1/\lambda_m + (1/\lambda_+ - 1/\lambda_-)p/(p^2 - 1)$ is the function-limiting point; and $\lambda_+ = 10^7/(0.831\cdot 10^7/\lambda_m + 7{,}070)$ and $\lambda_- = 10^7/(1.177\cdot 10^7/\lambda_m - 7{,}780)$ are the wavelength positions of half-maximal amplitudes. This formula was used to simulate the log-normal fluorescence spectra with various λ_{max} values (Figure 1).

Spectral moments of fluorescence spectra

Spectral moments and parameters for rotamer heterogeneity of Trp spectra were determined as follows:

1. Fluorescence spectra were acquired (305–500nm) of Trp in proteins using an excitation wavelength of 295 nm and corrected for light scattering and instrument response function.
2. The 280–305 nm region of corrected Trp spectra, was extrapolated from the log-normal function (usually one or two components) fit using formula (1) and the parameters obtained from the best fit using OriginPro version 8 (OriginLab Corp., Northampton, MA).
3. A composite spectrum was constructed. The region, 280–305 nm, was extrapolated from the fitting curve and added to the remainder of the corrected Trp spectra to obtain the composite full-width corrected spectra.
4. μ_1 and μ_2 values were calculated from the composite full-width corrected spectra using formula (2) and (3), respectively (see below).

$$\lambda_{mean}=\mu_1=\frac{\sum_i F_i\lambda_i}{\sum_i F_i} \quad (2)$$

$$\mu_2=\frac{\sum_i F_i(\lambda_i-\lambda_{mean})^2}{\sum_i F_i}=\frac{\sum_i F_i(\lambda_i^2-2\lambda_i\lambda_{mean}+\lambda_{mean}^2)}{\sum_i F_i}$$
$$=\frac{\sum_i F_i\lambda_i^2}{\sum_i F_i}-\frac{2\lambda_{mean}\sum_i F_i\lambda_i}{\sum_i F_i}+\frac{\lambda_{mean}^2\sum_i F_i}{\sum_i F_i}=\frac{\sum_i F_i\lambda_i^2}{\sum_i F_i}-2\lambda_{mean}^2+\lambda_{mean}^2=\frac{\sum_i F_i\lambda_i^2}{\sum_i F_i}-\lambda_{mean}^2 \quad (3)$$

where μ_1 and μ_2 are the first and second moments of fluorescence spectra, respectively. F_i is fluorescence intensity at each given wavelength (λ_i).

5. Formula (4) (see below) was used to calculate μ_2^* value for the “elementary” fluorescence spectrum corresponding to a particular λ_{max} value of the corrected spectra. Alternatively, one may generate the “elementary” fluorescence spectrum with a particular λ_{max} value and use the formula (3) to calculate μ_2^*.

$$\mu_2^*=\frac{1}{A+B\exp(-\lambda_{\max}/t)} \quad (4)$$

Reciprocals of the second moments of the "elementary" spectra depend exponentially on the fluorescence λ_{max} values and could be fit to formula 4 using OriginPro version 8 (OriginLab Corp., Northampton, MA). The best fits for parameters A, B and t were derived from simulated elementary log-normal components. μ_2^* is the second moment of the "elementary" fluorescence spectrum corresponding to a particular λ_{max} value.

6. Formula (5) below was used to calculate the spectral heterogeneity value.

The μ_2^* values were used to characterize rotamer heterogeneity of the fluorescence spectra of single Trp residues incorporated in various sites of the protein. We define rotamer heterogeneity as the degree of deviation from the corresponding "elementary" log-normal component, in the protein. Because the second moment depends on the fluorescence λ_{max}, rotamer heterogeneity of Trp fluorescence was scaled as

$$\Delta\mu_2=\frac{\mu_2-\mu_2^*}{\mu_2^*}\cdot 100\%. \quad (5)$$

As clear from the definition, single Trp fluorescence spectra with rotamer heterogeneity values close to 0 are well characterized with a single log-normal component.

Examples of single Trp fluorescence spectra for different class of proteins

To reliably compare spectral moment analysis, the literature was culled for single Trp fluorescence spectra that used λ_{ex} of 295 nm and were corrected for the instrument response function. The spectra were digitized using OriginPro version 8. The spectral data were interpolated to have 0.5 nm resolution. The digitized spectra were verified to match the original spectra.

Supplementary Material

Refer to Web version on PubMed Central for supplementary material.

Acknowledgments

This work was supported by U.S. Public Health Service grants NIH EY11224 (BG) and EY00331 (Core Grant) as well as the Edith and Lew Wasserman Endowed Professorship in Ophthalmology (B.G.).

Abbreviations

CD	circular dichroism
TL	tear lipocalin
SDTF	site-directed tryptophan fluorescence

References

1. Lakowicz, JR. Principles of Fluorescence Spectroscopy. 3. Springer; New York: 2006.
2. Herskovits TT, Sorensen M. Studies of the location of tyrosyl and tryptophyl residues in proteins. I. Solvent perturbation data of model compounds. Biochemistry. 1968; 7:2523–2532. [PubMed: 5660072]
3. Strickland EH. Aromatic contributions to circular dichroism spectra of proteins. CRC Crit Rev Biochem. 1974; 2:113–175. [PubMed: 4591332]
4. Grishina IB, Woody RW. Contributions of tryptophan side chains to the circular dichroism of globular proteins: exciton couplets and coupled oscillators. Faraday Discuss. 1994; 99:245–262. [PubMed: 7549540]
5. Gasymov OK, Abduragimov AR, Glasgow BJ. Site-directed circular dichroism of proteins: 1Lb bands of Trp resolve position-specific features in tear lipocalin. Anal Biochem. 2008; 374:386–395. [PubMed: 18047823]
6. Gasymov OK, Abduragimov AR, Yusifov TN, Glasgow BJ. Site-directed tryptophan fluorescence reveals the solution structure of tear lipocalin: evidence for features that confer promiscuity in ligand binding. Biochemistry. 2001; 40:14754–14762. [PubMed: 11732894]
7. Nagatomo S, Nagai M, Ogura T, Kitagawa T. Near-UV circular dichroism and UV resonance raman spectra of tryptophan residues as a structural marker of proteins. J Phys Chem B. 2013; 117:9343–9353. [PubMed: 23863193]
8. Gasymov OK, Abduragimov AR, Glasgow BJ. Double Tryptophan Exciton Probe to Gauge Proximal Side Chains in Proteins-Augmentation at Low Temperature. J Phys Chem B. 2015
9. Burstein EA, Abornev SM, Reshetnyak YK. Decomposition of protein tryptophan fluorescence spectra into log-normal components. I. Decomposition algorithms. Biophys J. 2001; 81:1699–1709. [PubMed: 11509382]
10. Reshetnyak YK, Burstein EA. Decomposition of protein tryptophan fluorescence spectra into log-normal components. II. The statistical proof of discreteness of tryptophan classes in proteins. Biophys J. 2001; 81:1710–1734. [PubMed: 11509383]
11. Reshetnyak YK, Koshevnik Y, Burstein EA. Decomposition of protein tryptophan fluorescence spectra into log-normal components. III. Correlation between fluorescence and microenvironment parameters of individual tryptophan residues. Biophys J. 2001; 81:1735–1758. [PubMed: 11509384]
12. Ladokhin AS, Jayasinghe S, White SH. How to measure and analyze tryptophan fluorescence in membranes properly, and why bother? Anal Biochem. 2000; 285:235–245. [PubMed: 11017708]
13. Shen C, Menon R, Das D, Bansal N, Nahar N, Guduru N, Jaegle S, Peckham J, Reshetnyak YK. The protein fluorescence and structural toolkit: Database and programs for the analysis of protein fluorescence and structural data. Proteins. 2008; 71:1744–1754. [PubMed: 18175321]
14. Hixon J, Reshetnyak YK. Algorithm for the analysis of tryptophan fluorescence spectra and their correlation with protein structural parameters. Algorithms. 2009; 2:1155–1176.
15. Lami H, Glasser N. Indole's solvatochromism revisited. J Chem Phys. 1986; 84:597–604.
16. Pierce DW, Boxer SG. Stark effect spectroscopy of tryptophan. Biophys J. 1995; 68:1583–1591. [PubMed: 7787044]
17. Callis PR, Burgess BK. Tryptophan fluorescence shifts in proteins from hybrid simulations: an electrostatic approach. J Phys Chem B. 1997; 101:9429–9432.
18. Callis PR, Tusell JR. MD + QM correlations with tryptophan fluorescence spectral shifts and lifetimes. Methods Mol Biol. 2014; 1076:171–214. [PubMed: 24108627]
19. Breustedt DA, Korndorfer IP, Redl B, Skerra A. The 1.8-A crystal structure of human tear lipocalin reveals an extended branched cavity with capacity for multiple ligands. J Biol Chem. 2005; 280:484–493. [PubMed: 15489503]
20. Gasymov OK, Abduragimov AR, Glasgow BJ. Tryptophan rotamer distribution revealed for the alpha-helix in tear lipocalin by site-directed tryptophan fluorescence. J Phys Chem B. 2012; 116:13381–13388. [PubMed: 23088798]

21. Gasymov OK, Abduragimov AR, Glasgow BJ. Effect of short- and long-range interactions on trp rotamer populations determined by site-directed tryptophan fluorescence of tear lipocalin. PLoS One. 2013; 8:e78754. [PubMed: 24205305]
22. Burstein EA, Emelyanenko VI. Log-normal description of fluorescence spectra of organic fluorophores. Photochem Photobiol. 1996; 64:316–320.
23. Callis PR. Binding phenomena and fluorescence quenching. I: Descriptive quantum principles of fluorescence quenching using a supermolecule approach. J Mol Struct. 2014; 1077:14–21.
24. Tusell JR, Callis PR. Computational predictions of exponential and non-exponential tryptophan fluorescence decay in NATA, the villin headpiece subdomain, and other proteins. Biophys J. 2012; 102:217a.
25. Royer CA, Weber G, Daly TJ, Matthews KS. Dissociation of the lactose repressor protein tetramer using high hydrostatic pressure. Biochemistry. 1986; 25:8308–8315. [PubMed: 3545291]
26. Otosu T, Nishimoto E, Yamashita S. Multiple conformational state of human serum albumin around single tryptophan residue at various pH revealed by time-resolved fluorescence spectroscopy. J Biochem. 2010; 147:191–200. [PubMed: 19884191]
27. Pattanaik P, Ravindra G, Sengupta C, Maithal K, Balaram P, Balaram H. Unusual fluorescence of W168 in Plasmodium falciparum triosephosphate isomerase, probed by single-tryptophan mutants. Eur J Biochem. 2003; 270:745–756. [PubMed: 12581214]
28. Siano DB, Metzler DE. Band shapes of the electronic spectra of complex molecules. J Chem Phys. 1969; 51:1856–1861.
29. Vivian JT, Callis PR. Vibronic band shapes for indole from scaled bond order changes. Chem Phys Lett. 1994; 229:153–I 160.
30. Schiffer M, Chang CH, Stevens FJ. The functions of tryptophan residues in membrane proteins. Protein Eng. 1992; 5:213–214. [PubMed: 1409540]
31. Flower DR. The lipocalin protein family: structure and function. Biochem J. 1996; 318(Pt 1):1–14. [PubMed: 8761444]
32. Flower DR, North AC, Sansom CE. The lipocalin protein family: structural and sequence overview. Biochim Biophys Acta. 2000; 1482:9–24. [PubMed: 11058743]
33. Gasymov OK, Abduragimov AR, Yusifov TN, Glasgow BJ. Binding studies of tear lipocalin: the role of the conserved tryptophan in maintaining structure, stability and ligand affinity. Biochim Biophys Acta. 1999; 1433:307–320. [PubMed: 10515687]
34. Tilstra L, Sattler MC, Cherry WR, Barkley MD. Fluorescence of a rotationally constrained tryptophan derivative, 3-carboxy-1,2,3,4-tetrahydro-2-carboline. J Am Chem Soc. 1990; 112:9176–9182.
35. Chen Y, Barkley MD. Toward understanding tryptophan fluorescence in proteins. Biochemistry. 1998; 37:9976–9982. [PubMed: 9665702]
36. Chen Y, Liu B, Yu HT, Barkley MD. The peptide bond quenches indole fluorescence. J Am Chem Soc. 1996; 118:9271–9278.
37. Pan CP, Muino PL, Barkley MD, Callis PR. Correlation of tryptophan fluorescence spectral shifts and lifetimes arising directly from heterogeneous environment. J Phys Chem B. 2011; 115:3245–3253. [PubMed: 21370844]
38. Callis PR, Liu T. Quantitative prediction of fluorescence quantum yields for tryptophan in proteins. J Phys Chem B. 2004; 108:4248–4259.
39. Callis PR, Petrenko A, Muino PL, Tusell JR. Ab initio prediction of tryptophan fluorescence quenching by protein electric field enabled electron transfer. J Phys Chem B. 2007; 111:10335–10339. [PubMed: 17696529]
40. Adams PD, Chen Y, Ma K, Zagorski MG, Sonnichsen FD, McLaughlin ML, Barkley MD. Intramolecular quenching of tryptophan fluorescence by the peptide bond in cyclic hexapeptides. J Am Chem Soc. 2002; 124:9278–9286. [PubMed: 12149035]
41. Liu B, Thalji RK, Adams PD, Fronczek FR, McLaughlin ML, Barkley MD. Fluorescence of cis-1-amino-2-(3-indolyl)cyclohexane-1-carboxylic acid: a single tryptophan chi(1) rotamer model. J Am Chem Soc. 2002; 124:13329–13338. [PubMed: 12405862]
42. Pan CP, Barkley MD. Conformational effects on tryptophan fluorescence in cyclic hexapeptides. Biophys J. 2004; 86:3828–3835. [PubMed: 15189879]

43. Dedonder-Lardeux C, Jouvet C, Perun S, Sobolewski AL. External electric field effect on the lowest excited states of indole: ab initio and molecular dynamics study. Phys Chem Chem Phys. 2003; 5
44. Albani JR, Vogelaer J, Bretesche L, Kmiecik D. Tryptophan 19 residue is the origin of bovine beta-lactoglobulin fluorescence. J Pharm Biomed Anal. 2014; 91:144–150. [PubMed: 24463042]
45. Albani JR. Fluorescence lifetimes of tryptophan: structural origin and relation with So --> 1Lb and So --> 1La transitions. J Fluoresc. 2009; 19:1061–1071. [PubMed: 19533308]
46. Albani JR. Origin of tryptophan fluorescence lifetimes part 1. Fluorescence lifetimes origin of tryptophan free in solution. J Fluoresc. 2014; 24:93–104. [PubMed: 23912963]
47. Albani JR. Origin of tryptophan fluorescence lifetimes. Part 2: fluorescence lifetimes origin of tryptophan in proteins. J Fluoresc. 2014; 24:105–117. [PubMed: 23907253]
48. Pan CP, Callis PR, Barkley MD. Dependence of tryptophan emission wavelength on conformation in cyclic hexapeptides. J Phys Chem B. 2006; 110:7009–7016. [PubMed: 16571015]
49. Broos J, Tveen-Jensen K, de Waal E, Hesp BH, Jackson JB, Canters GW, Callis PR. The emitting state of tryptophan in proteins with highly blue-shifted fluorescence. Angew Chem Int Ed Engl. 2007; 46:5137–5139. [PubMed: 17539030]
50. Callis PR. 1La and 1Lb transitions of tryptophan: applications of theory and experimental observations to fluorescence of proteins. Methods Enzymol. 1997; 278:113–150. [PubMed: 9170312]
51. Vivian JT, Callis PR. Mechanisms of tryptophan fluorescence shifts in proteins. Biophys J. 2001; 80:2093–2109. [PubMed: 11325713]
52. Gasymov OK, Abduragimov AR, Glasgow BJ. pH-Dependent conformational changes in tear lipocalin by site-directed tryptophan fluorescence. Biochemistry. 2010; 49:582–590. [PubMed: 20025287]
53. Gasymov OK, Abduragimov AR, Glasgow BJ. Excited protein states of human tear lipocalin for low- and high-affinity ligand binding revealed by functional AB loop motion. Biophys Chem. 2010; 149:47–57. [PubMed: 20439130]
54. Gasymov OK, Abduragimov AR, Yusifov TN, Glasgow BJ. Resolution of ligand positions by site-directed tryptophan fluorescence in tear lipocalin. Protein Sci. 2000; 9:325–331. [PubMed: 10716184]
55. Gasymov OK, Abduragimov AR, Yusifov TN, Glasgow BJ. Interstrand loops CD and EF act as pH-dependent gates to regulate fatty acid ligand binding in tear lipocalin. Biochemistry. 2004; 43:12894–12904. [PubMed: 15461462]
56. Colucci WJ, Tilstra L, Sattler MC, Fronczek FR, Barkley MD. Conformational studies of a constrained tryptophan derivative: implications for the fluorescence quenching mechanism. J Am Chem Soc. 1990; 112:9182–9190.
57. McMahon LP, Yu HT, Vela MA, Morales GA, Shui L, Fronczek FR, McLaughlin ML, Barkley MD. Conformer Interconversion in the Excited State of Constrained Tryptophan Derivatives. J Phys Chem B. 1997; 101:3269–3280.
58. Gasymov OK, Abduragimov AR, Glasgow BJ. Probing tertiary structure of proteins using single Trp mutations with circular dichroism at low temperature. J Phys Chem B. 2014
59. Breustedt DA, Chatwell L, Skerra A. A new crystal form of human tear lipocalin reveals high flexibility in the loop region and induced fit in the ligand cavity. Acta Crystallogr D Biol Crystallogr. 2009; 65:1118–1125. [PubMed: 19770509]
60. Gasymov OK, Abduragimov AR, Glasgow BJ. Cation-pi interactions in lipocalins: structural and functional implications. Biochemistry. 2012; 51:2991–3002. [PubMed: 22439821]
61. Amiri M, Jankeje K, Albani JR. Characterization of human serum albumin forms with pH. Fluorescence lifetime studies. J Pharm Biomed Anal. 2010; 51:1097–10102. [PubMed: 20005063]
62. Lakowicz JR. On spectral relaxation in proteins. Photochem Photobiol. 2000; 72:421–437. [PubMed: 11045710]
63. Redl B, Holzfeind P, Lottspeich F. cDNA cloning and sequencing reveals human tear prealbumin to be a member of the lipophilic-ligand carrier protein superfamily. J Biol Chem. 1992; 267:20282–20287. [PubMed: 1400345]

64. Glasgow BJ, Heinzmann C, Kojis T, Sparkes RS, Mohandas T, Bateman JB. Assignment of tear lipocalin gene to human chromosome 9q34-9qter. Curr Eye Res. 1993; 12:1019–1023. [PubMed: 8306712]

65. Glasgow BJ. Tissue expression of lipocalins in human lacrimal and von Ebner's glands: colocalization with lysozyme. Graefes Arch Clin Exp Ophthalmol. 1995; 233:513–522. [PubMed: 8537027]

66. Berengian AR, Bova MP, McHaourab HS. Structure and function of the conserved domain in alphaA-crystallin. Site-directed spin labeling identifies a beta-strand located near a subunit interface. Biochemistry. 1997; 36:9951–9957. [PubMed: 9296605]

67. Glasgow BJ, Abduragimov AR, Farahbakhsh ZT, Faull KF, Hubbell WL. Tear lipocalins bind a broad array of lipid ligands. Curr Eye Res. 1995; 14:363–372. [PubMed: 7648862]

68. Tsukamoto S, Fujiwara K, Ikeguchi M. Fatty acids bound to recombinant tear lipocalin and their role in structural stabilization. J Biochem. 2009; 146:343–350. [PubMed: 19470520]

69. Gasymov OK, Abduragimov AR, Glasgow BJ. The conserved disulfide bond of human tear lipocalin modulates conformation and lipid binding in a ligand selective manner. Biochim Biophys Acta. 2011; 1814:671–683. [PubMed: 21466861]

70. Albani JR. Relation between proteins tertiary structure, tryptophan fluorescence lifetimes and tryptophan S(o)-->(1)L(b) and S(o)-->(1)L(a) transitions. Studies on alpha1-acid glycoprotein and beta-lactoglobulin. J Fluoresc. 2011; 21:1301–1309. [PubMed: 21318433]

Appendix A. Supplementary material

Supplementary data associated with this article can be found in the online version.

Highlights

- The blue side Trp emission is extrapolated from log-normal analysis.
- Spectral moments reflect the site-resolved secondary structure of the proteins.
- Second spectral moments reveal enhanced heterogeneity in specific sites.
- Spectral heterogeneity values characterize inhomogeneous broadening.
- Site-specific spectral heterogeneity fits the internal Stark effect for rotamers.

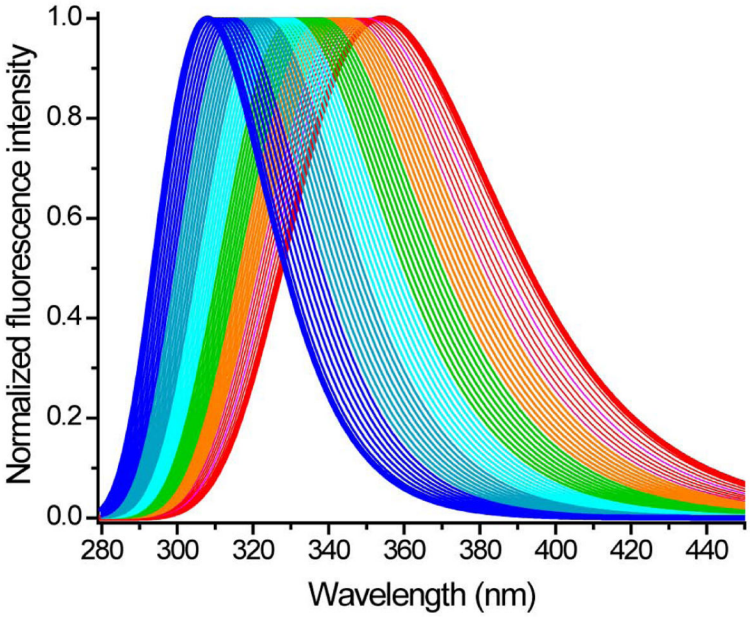

Figure 1.

Simulated log-normal fluorescence spectra of Trp with various λ_{max} values. Normalized fluorescence spectra are derived from parameters and the formula described in the experimental methods section. The blue shift decreases the bandwidth of the spectrum.

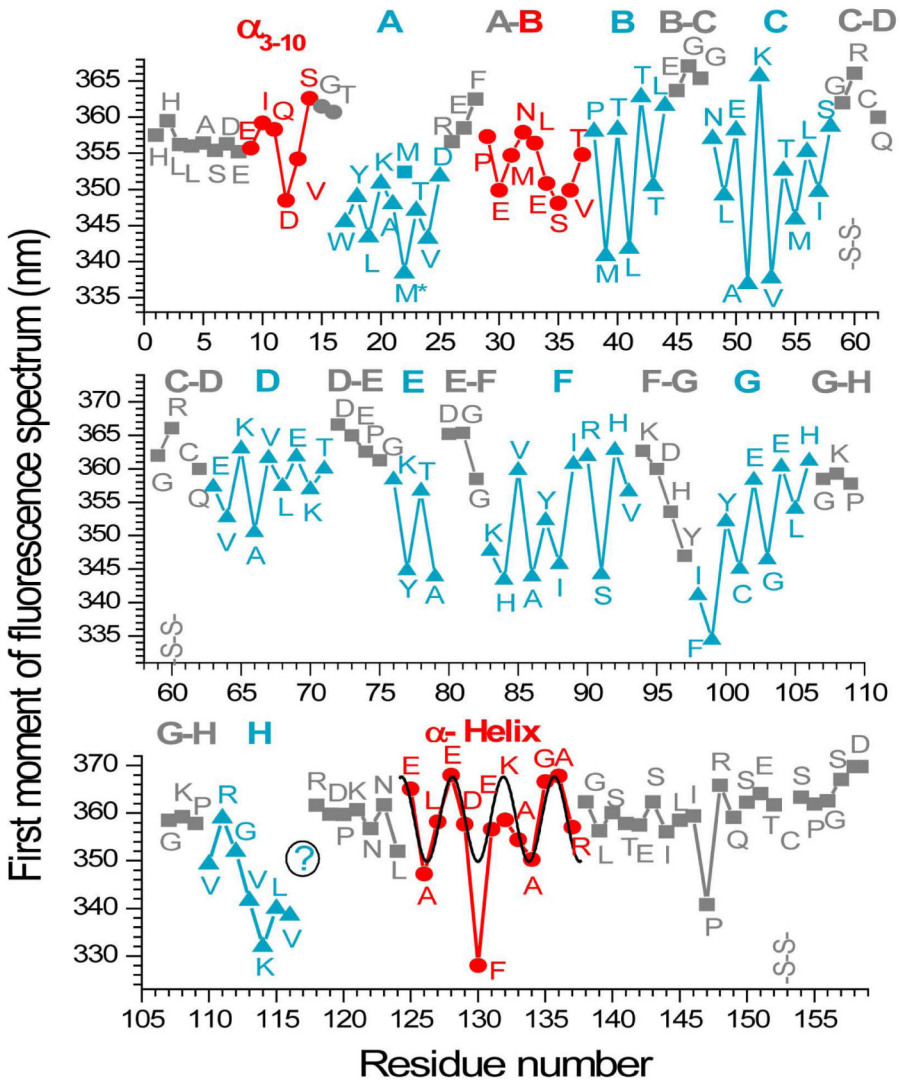

Figure 2.

The first moments of the corrected spectra of single Trp mutants of TL. The sites for the *β*-strand and α-helix regions are shown in blue triangles and red circles, respectively. Gray squares represent amino acid residue sites without secondary structure such as in some areas of loops. Single bold letters refer to *β*-strands (e.g., A is the *β*-strand A). Loops are designated by two letters of the connecting strands (e.g., A–B is the loop between the *β*-strands A and B). The A–B loop is depicted by gray and red letters to indicate some α-helical content. The solid black line is the fitting curve (periodicity of 3.6) for α-helical content. The question mark is shown for position 117 because mutant G117W could not be expressed or purified in a monomeric state. M* is the first moment for M22W/K114C. The disulfide bond joining 61–151 is denoted as S-S.

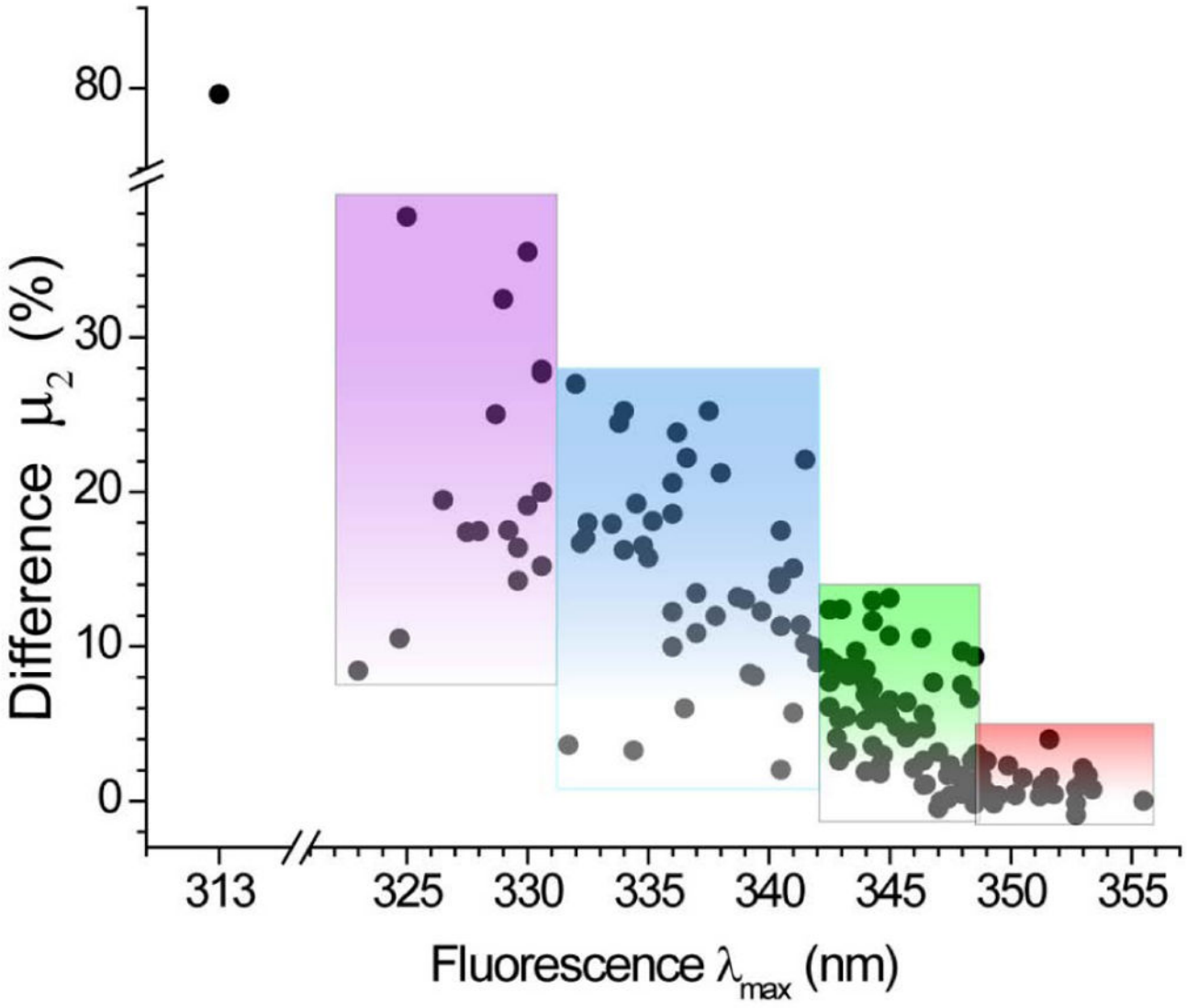

Figure 3.

Dependence of rotamer heterogeneity value ($\Delta\mu_2$) on fluorescence λ_{max} values in TL. The rotamer heterogeneity values can be grouped according to their distribution as represented by the various colors. For example, rotamer heterogeneity is minimal for greatly red shifted λmax values, represented by the red color.

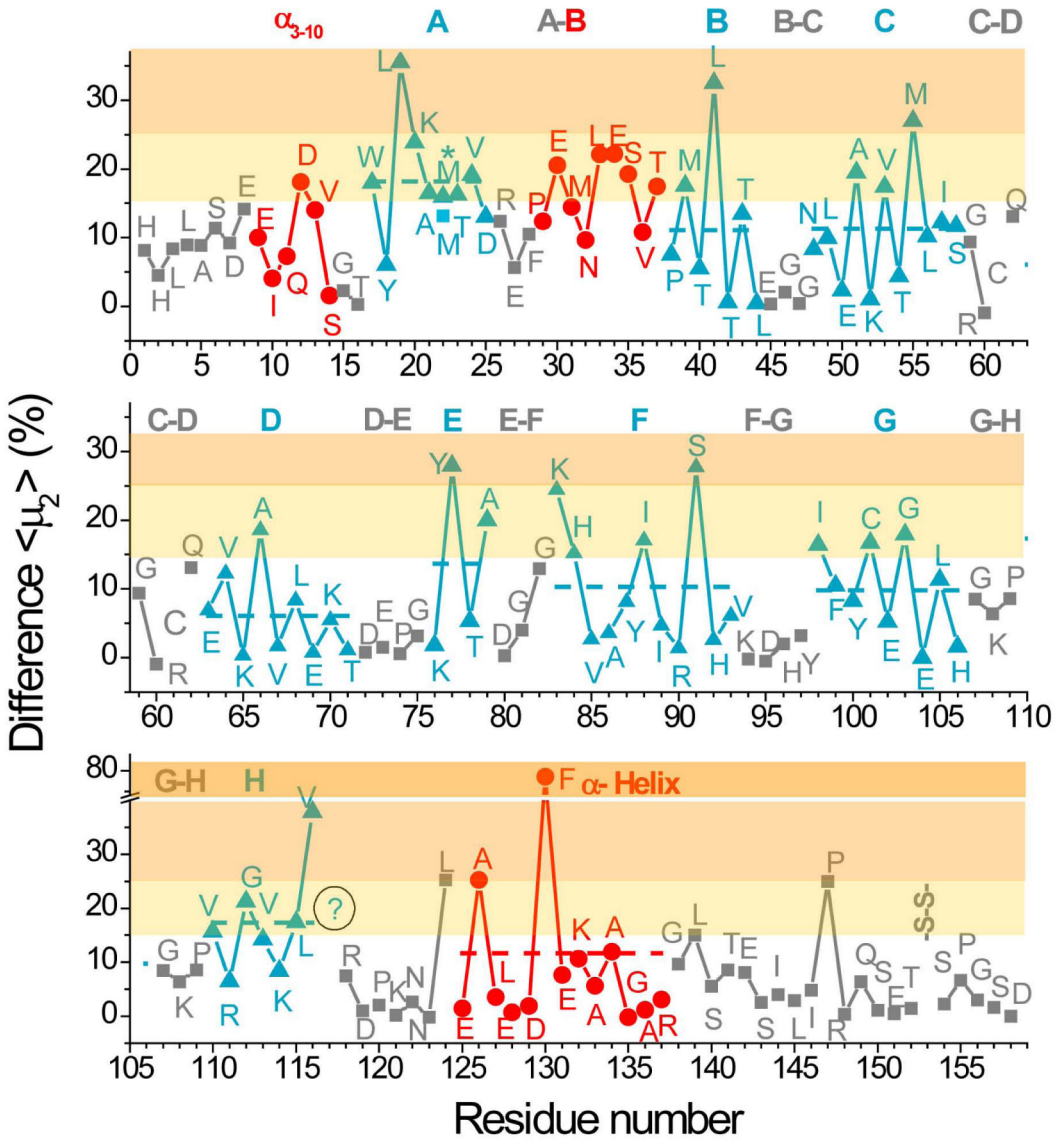

Figure 4.

The rotamer heterogeneity of the corrected spectra of single Trp mutants of TL plotted sequentially along the amino acid sequence. The letters, symbols and color schemes are identical to that of Figure 2. Horizontal dashed lines represent average rotamer heterogeneity for the assigned secondary structure regions. Colored horizontal lanes indicate defined rotamer heterogeneity regions, 15–25, 25–40 and >40.

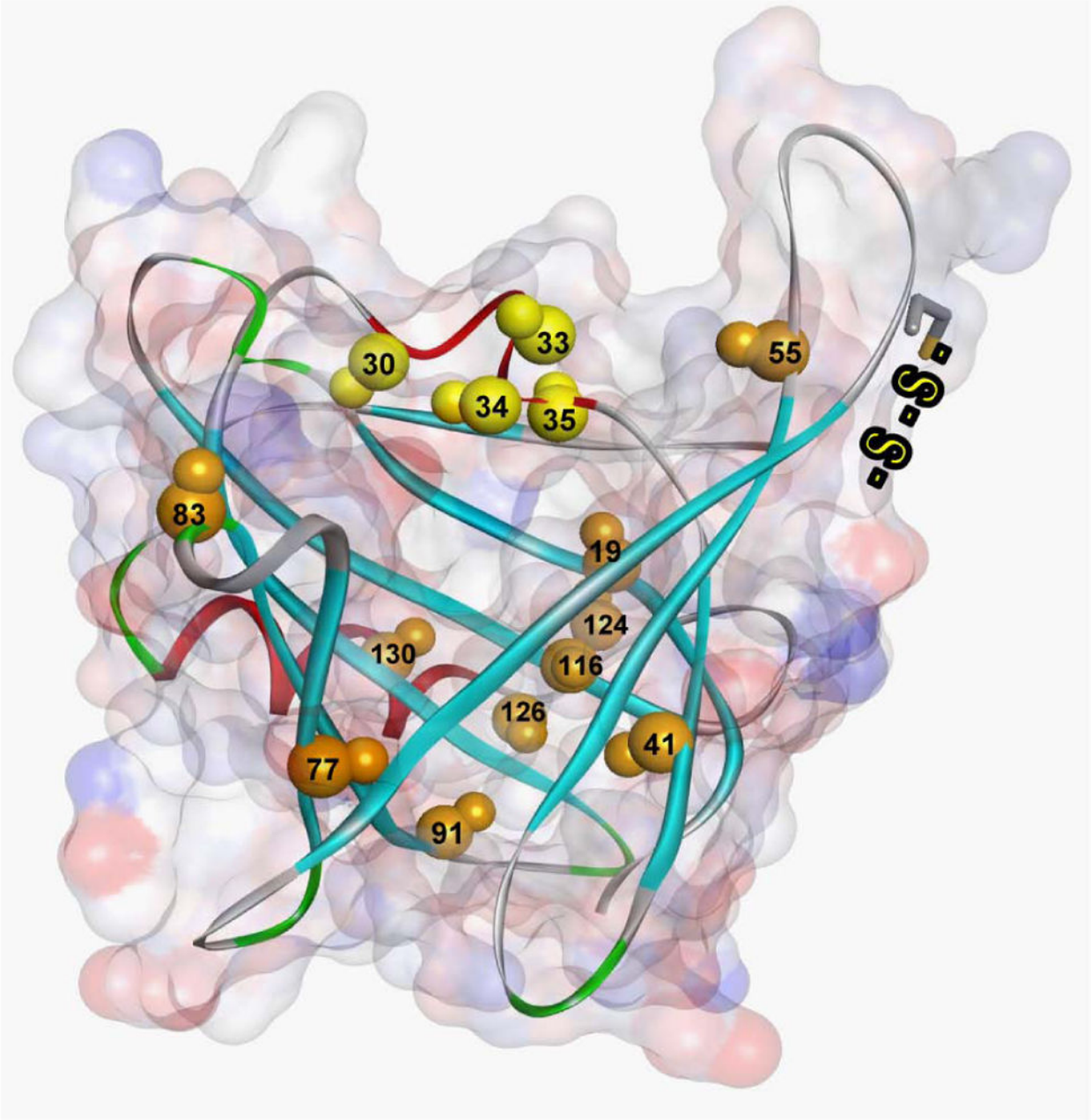

Figure 5.

Sites in TL with the highest rotamer heterogeneity for Trp fluorescence. Large and small spheres show locations of the C^{α}- and C^{β}- atoms, respectively, of the amino acid residues. Brown colored spheres represent sites with the highest rotamer heterogeneity in TL (>25, see Method for definition). Yellow colored spheres show sites in loops with the highest rotamer heterogeneity (15–24). Amino acid positions are numbered in sequence. Cys61 but not Cys 153 of the disulfide bond is resolved in the crystal structure. The native disulfide bond is indicated by the letter adjacent to the side chain of Cys61. The ribbon diagram (blue for β-strands, red for α-helix, green for turns, and gray for loops) of TL was generated from

Protein Data Bank entry 1XKI with DS Visualizer 3.5 (Accelrys Inc.). Missing loop fragments (part of the loops AB and GH) were modeled using DeepView/Swiss-PdbViewer version 3.7 (GlaxoSmithKline R&D) in accord with solution structure data (Figure 2 and the reference [6]). The surface representation is colored according to the electrostatic potential, blue for positive charge and red for negative).

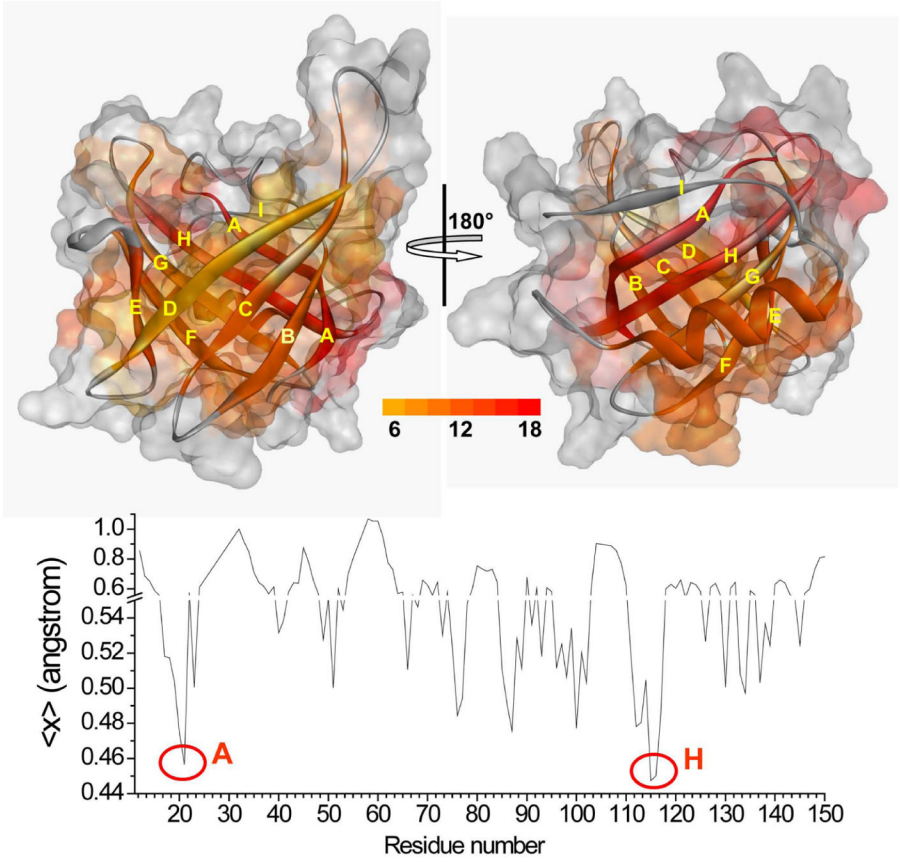

Figure 6.

Ribbon diagrams of TL that show the degree of rotamer heterogeneity for secondary structural elements. Each ribbon drawing of the β-stands and α-helix of TL is colored according the average degree rotamer heterogeneity for a particular secondary structural element (color scale shown). Gray color represents regions where rotamer heterogeneity is not specified. The letters denote the identities of the β-strands. The mean isotropic displacement of the Cα-atoms for each residue were calculated from the crystallographic B-factor parameters (shown in the lower part of the figure). Circles and letters highlight the β-strands that possess the lowest mean displacements. The figure was generated as indicated in the figure legend 5.

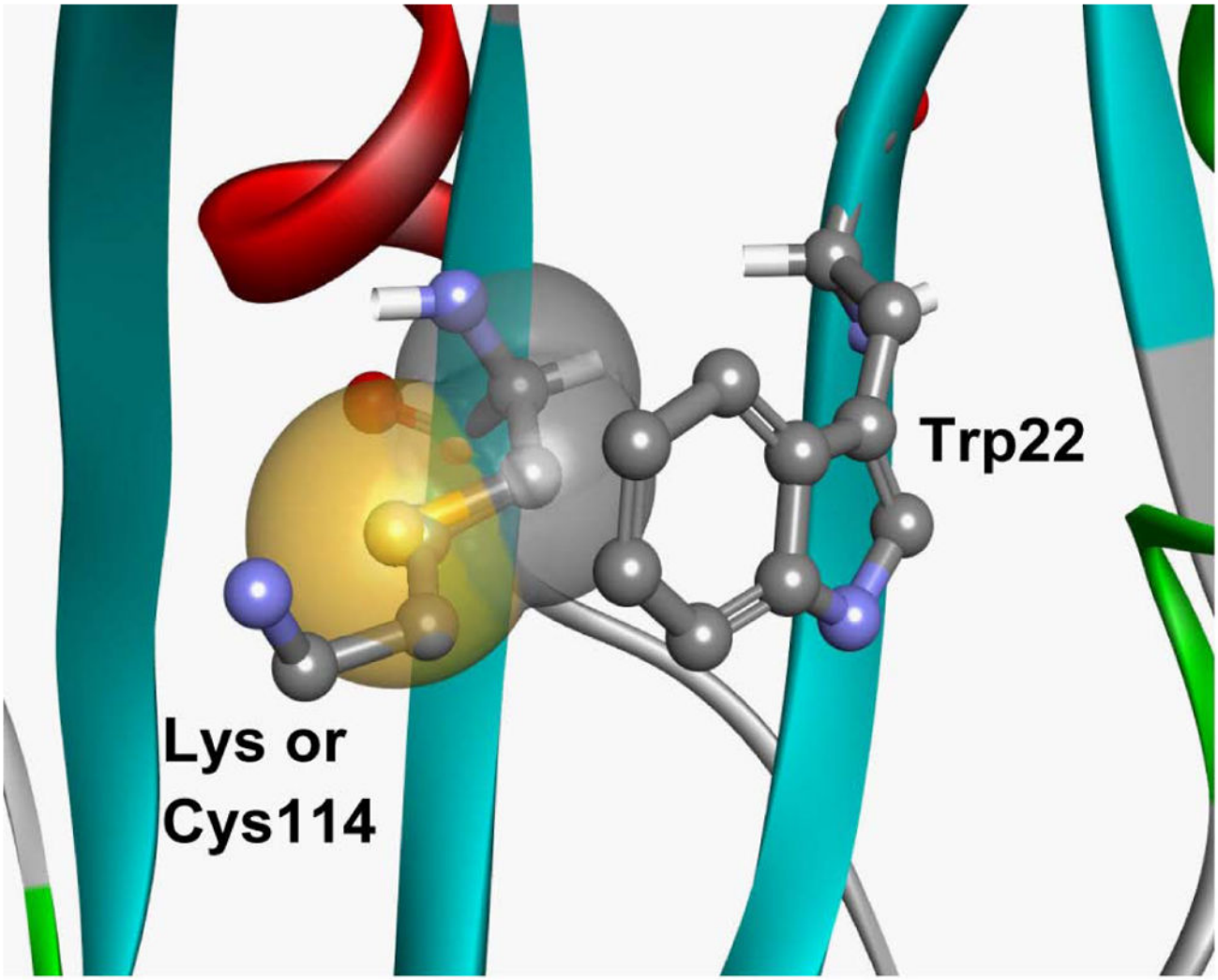

Figure 7.

The orientation of the positively charged residue Lys114 relative to Trp 22. The side chain of Cys114 is overlapped with native Lys. For visual guidance the side chain atoms of Cys114 was also represented in spheres. The figure was generated from Protein Data Bank entry 1XKI.

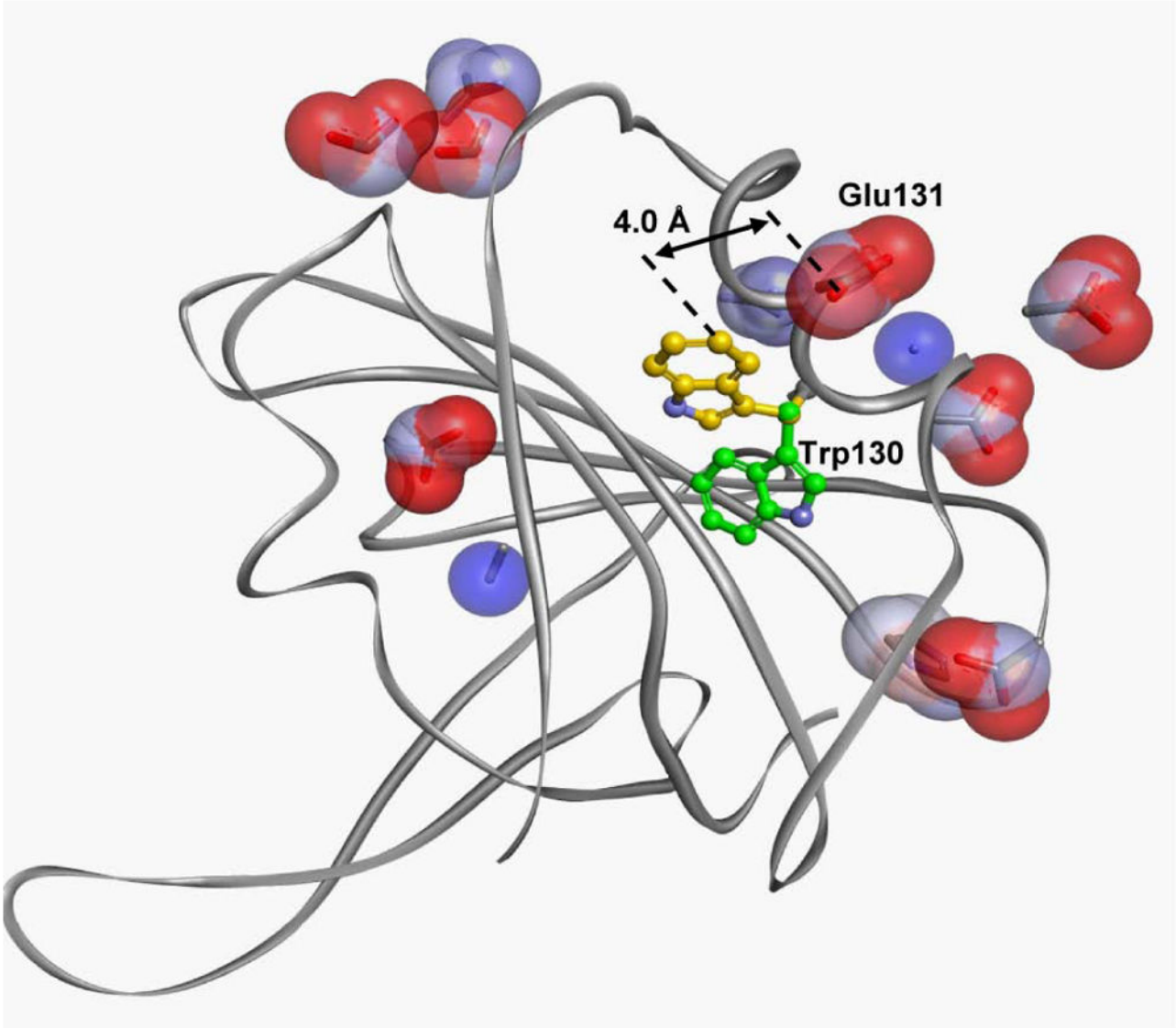

Figure 8.

Charged residues (within 12 Å) around mutation at Trp130. The predominant *t*- (yellow carbon atoms) and g^- (golden carbon atoms) rotamers, were determined from fluorescence lifetime measurements [20]. The distance between the C4 atom of the indole (*t*-rotamer) and oxygen atom (indicated) of Glu 131 is 4.0 Å, which is the closest charged atom. The figure was generated as indicated in the figure legend 5.

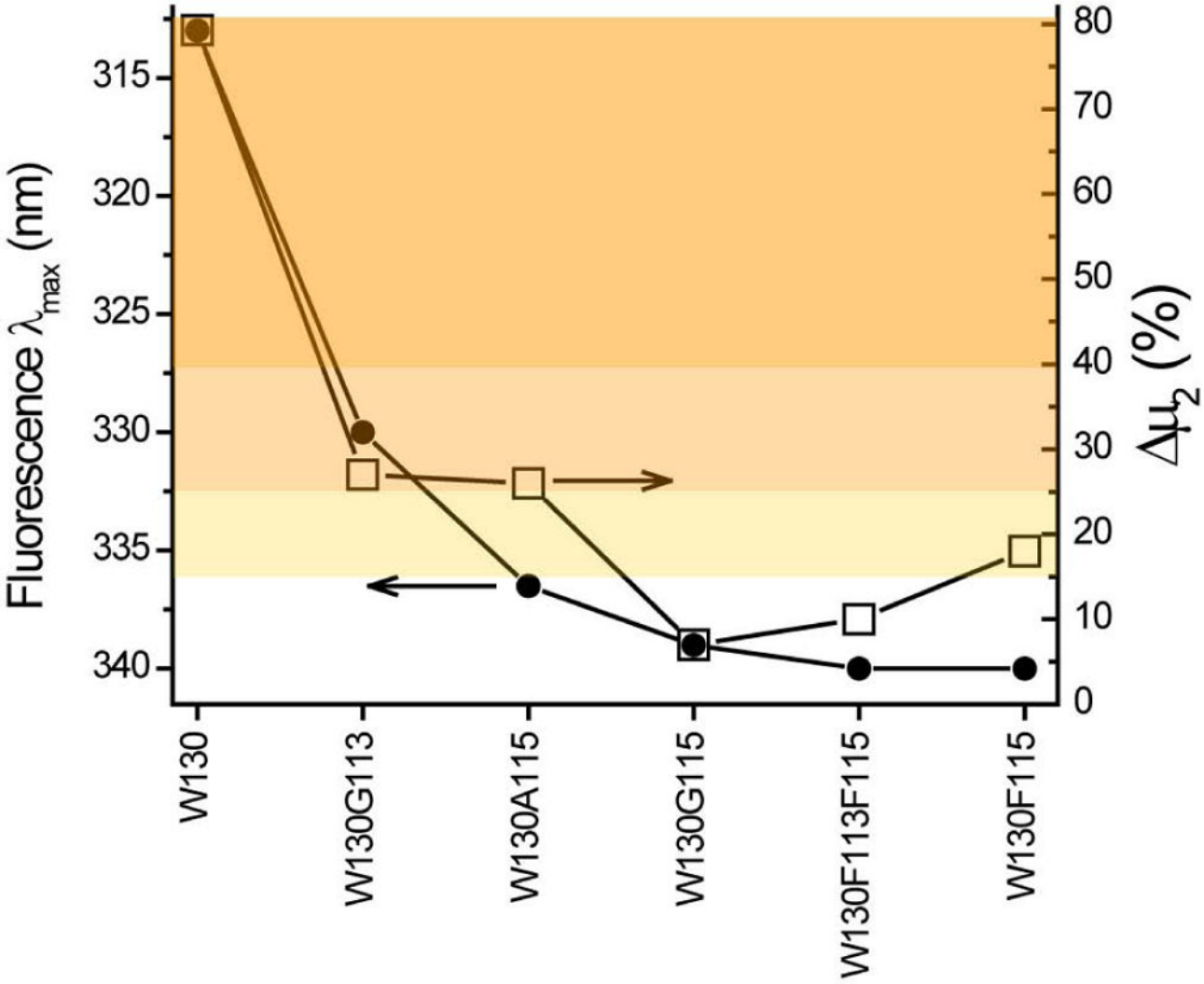

Figure 9.

Influence of long-range interaction to fluorescence maxima and spectral rotamer heterogeneity. Trp130 and its interaction sites V113 and L115 are chosen as an example. The solid circles represent fluorescence λmax values for the respective mutants. The open rectangles are the rotamer heterogeneity values for the relevant mutants. Figure 10. Distribution of occurrence of Trp fluorescence λ_{max} values in all sites of TL (blackbars) and in about 150 proteins (gray bars, graph is adapted from the reference [13].

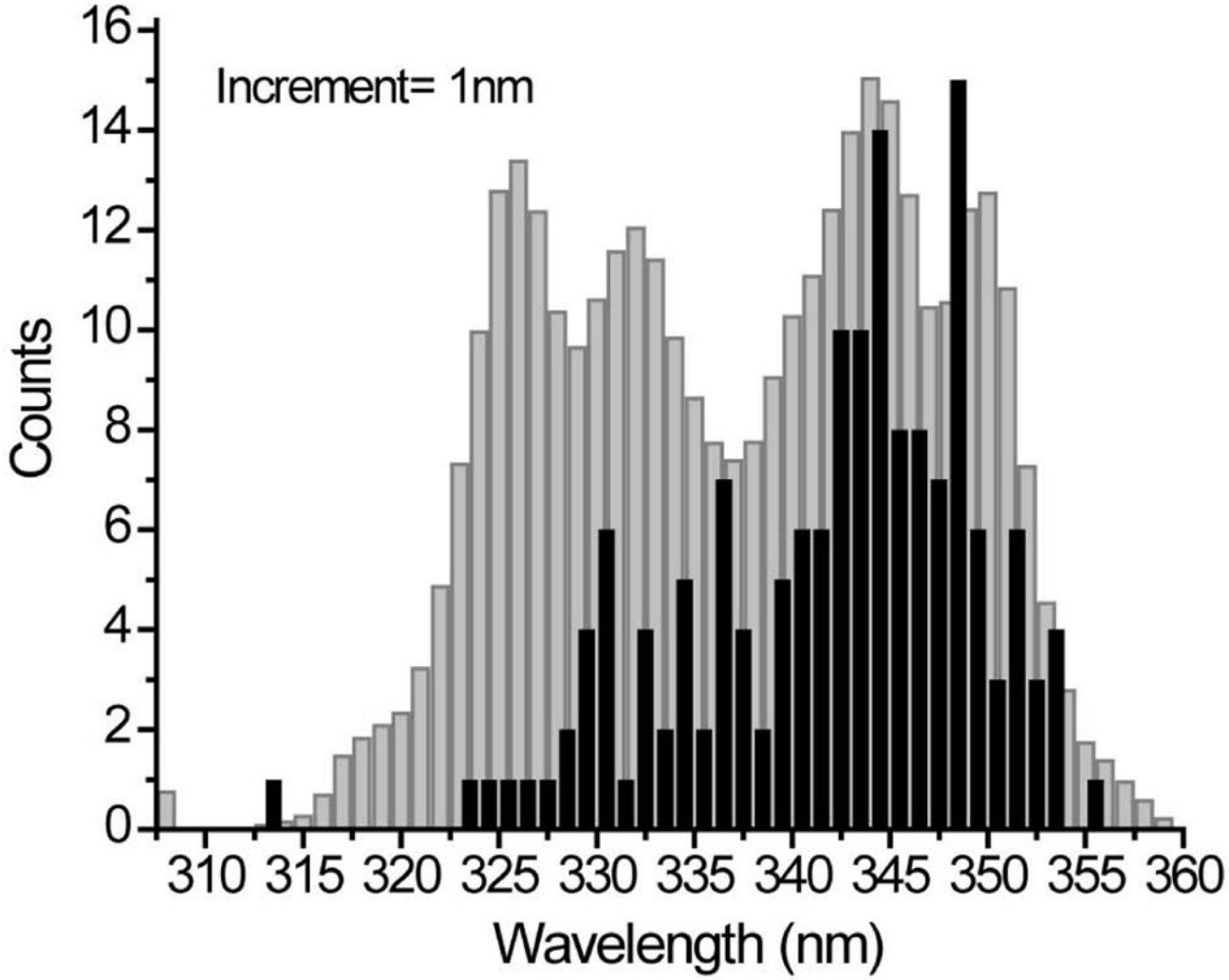

Figure 10.
Distribution of occurrence of Trp fluorescence λ_{max} values in all sites of TL (black bars) and in about 150 proteins (gray bars, graph is adapted from reference 13.

Table 1

Fluorescence parameters calculated from constructed full scale emission spectra for single Trp residues in various proteins.

Protein	Fluorescence λmax (nm)	μ_1 (nm)	μ_2 (nm^2)	$\Delta\mu_2$ (%)	Data Source
bovine β-lactoglobulin	332.5	344.2	773	18	[44]
bovine β-lactoglobulin	332.5	344.2	743	13	[70]
HSA, pH 2.0	336.5	350.4	939	27	[26]
HSA, pH 4.1	340	353.6	1006	28	[26]
HSA, pH 7.0	348	360.2	1077	15	[26]
HSA, pH 9.0	346	358.1	1061	17	[26]
PfTIM (Trp 168)	329	346.6	1028	72	[27]
PfTIM (Trp 11)	333	348.4	952	43	[27]

Table 2

Average fluorescence decay parameters of W214 in HSA at various pH values calculated from Table 1 of reference [26].

pH	α_1	α_2	α_3	τ_1 (ns)	τ_2 (ns)	τ_3 (ns)	f_1	f_2	f_3
2.0	0.49	0.34	0.17	5.54	2.05	0.40	0.81	0.18	0.02
4.1	0.59	0.29	0.12	6.46	2.77	0.41	0.86	0.13	0.01
7.0	0.62	0.29	0.10	7.51	3.41	0.20	0.911	0.087	0.002
9.0	0.64	0.22	0.14	6.55	2.48	0.33	0.926	0.069	0.006